NONDESTRUCTIVE PERMITTIVITY AND LOSS TANGENT MEASUREMENTS WITH A SPLIT-CYLINDER RESONATOR*

Michael Janezic[(1)], Edward Kuester[(2)], James Baker-Jarvis[(1)]

[(1)] ***National Institute of Standards and Technology, Boulder, Colorado, USA 80305***
[(2)] ***University of Colorado, Electrical and Computer Engineering, Boulder Colorado, USA 80309***

ABSTRACT

We present a new theoretical model, based on the mode-matching method, for performing nondestructive permittivity and loss tangent measurements with the split-cylinder resonator. This new model properly takes into account the fringing electric and magnetic fields, thereby improving the measurement accuracy of the technique. In order to verify the new split-cylinder model, we present measurements of permittivity and loss tangent for several dielectric substrates and show good agreement with measurements made in a conventional cylindrical cavity.

INTRODUCTION

The split-cylinder resonator technique is a nondestructive method for measuring the permittivity and loss tangent of low-loss dielectric substrates. Originally proposed by Kent [1, 2], this method employs a cylindrical cavity, that is separated into two halves, as shown in Fig. 1. A sample is placed in the gap between the two shorted cylindrical waveguide sections. A coupling loop in each waveguide section excites a TE_{011} resonance, and from measurements of the resonant frequency and quality factor, the permittivity and loss tangent of the sample can be determined.

The advantage of the split-cylinder method is that the sample needs only to be planar and extend sufficiently far beyond the diameter of the two cylindrical waveguide sections. No other sample machining is necessary, making this method attractive for accurate, nondestructive measurements of low-loss substrates. Unfortunately, having little or no sample preparation comes at the cost of needing a more complicated model. For the case of the split-cylinder, the model must include the electric and magnetic fields that extend into the sample region beyond the cylindrical waveguide regions. In order to obtain accurate measurements of permittivity and loss tangent, these fields must be accurately determined.

Previously [3] we developed a theoretical model employing Hankel transforms that rigorously took into account these fringing fields and improved the accuracy of the permittivity measurements. From this theoretical model we derived a resonance condition for the split-cylinder resonator for calculating the sample permittivity. Although accurate, this new model was computationally intensive, so we have developed a new theoretical model for the split-cylinder resonator, based on the mode-matching method. Using this model, we derive equations for calculating the relative permittivity and loss tangent of a sample. In this paper, we summarize this new theoretical model and show how to use the resulting equations to calculate the sample permittivity and loss tangent. In order to verify the new split-cylinder theoretical model, we also compare measurements made on three dielectric materials with measurements made with another accurate technique, the 10 GHz cylindrical cavity.

RELATIVE PERMITTIVITY

In our initial model for calculating the sample permittivity, we assumed that the sample extended to infinity in the radial direction [3]. However, if the fringing electric and magnetic fields decrease as a function of ρ in the sample region, we may assume that a perfect conductor exists at some sufficiently large $\rho = b$, without introducing a systematic error in the calculation of the sample permittivity and loss tangent. By introducing this boundary, we enclose the entire split-cylinder resonator fixture, and derive a new model based on the mode-matching method.

Assuming TE_{0n} mode excitation, we determined the transverse electric and magnetic fields in the upper cylindrical waveguide region from Maxwell's equations and enforcement of the boundary conditions on the upper waveguide endplate and walls:

$$E_{\phi_u}(\rho,z) = \sum_{n=1}^{N_u} A_n U_n J_1(h_{n_u}\rho)\sin\left[p_{n_u}\left(L+\frac{d}{2}-z\right)\right] \tag{1}$$

$$H_{\rho_u}(\rho,z) = -\frac{1}{j\omega\mu_0}\sum_{n=1}^{N_u} A_n U_n p_{n_u} J_1(h_{n_u}\rho)\cos\left[p_{n_u}\left(L+\frac{d}{2}-z\right)\right], \tag{2}$$

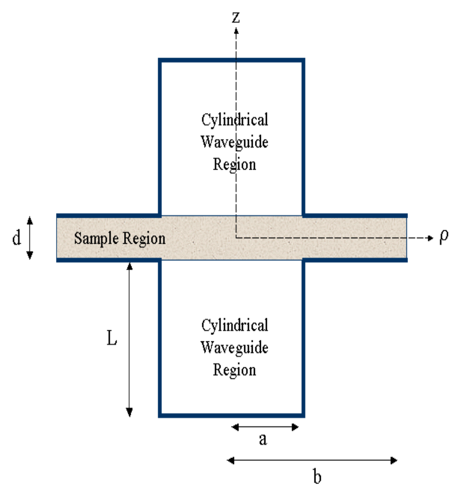

Figure 1: Cross-sectional diagram of a split-cylinder resonator.

where $p_{n_u}^2 = k_u^2 - h_{n_u}^2$, $k_u^2 = \omega^2 \mu_0 \epsilon_0 \epsilon_a^{'}$, $h_{n_u} = \frac{j_{1,n}}{a}$, A_n are constants to be determined, and N_u is the total number of modes included in the upper waveguide region. Additional geometrical parameters are given in Fig. 1. We have included the factors $U_n = p_{N_u} / \cosh\left[\mathrm{Im}(p_{n_u})L\right]$ to improve matrix conditioning.

Since the sample region is also enclosed by a perfect conductor at $\rho = b$, we express the transverse electric and magnetic fields in the sample region in a similar manner:

$$E_{\phi_s}(\rho, z) = \sum_{n=1}^{N_s} B_n V_n J_1(h_{n_s}\rho) \cos(p_{n_s} z) \tag{3}$$

$$H_{\rho_s}(\rho, z) = -\frac{1}{j\omega\mu_0} \sum_{n=1}^{N_s} B_n V_n p_{n_s} J_1(h_{n_s}\rho) \sin(p_{n_s} z), \tag{4}$$

where $p_{n_s}^2 = k_s^2 - h_{n_s}^2$, $k_s^2 = \omega^2 \mu_0 \epsilon_0 \epsilon_s^{'}$, $h_{n_s} = \frac{j_{1,n}}{b}$, B_n are constants to be determined, and N_s is the total number of modes included in the sample region. In this case, we included the terms $V_n = p_{N_s} / \cosh\left[\mathrm{Im}(p_{n_s})\frac{d}{2}\right]$ to improve matrix conditioning.

We derive a resonance condition by enforcing the boundary conditions for the transverse electric and magnetic field. The tangential electric and magnetic fields are continuous at $z = d/2$:

$$E_{\phi_u}\left(z = \frac{d}{2}\right) = E_{\phi_s}\left(z = \frac{d}{2}\right) \quad 0 \le \rho \le b, \tag{5}$$

$$H_{\rho_u}\left(z = \frac{d}{2}\right) = H_{\rho_s}\left(z = \frac{d}{2}\right) \quad 0 \le \rho \le a. \tag{6}$$

Substituting the series electric and magnetic field representations (1-4) into (5) and (6), multiplying each side by the electric or magnetic field [H_{ρ_s} in the case of (5), E_{ϕ_u} in the case of (6)], integrating over the appropriate cross-section, and employing orthogonality of the modes [4], we obtain two systems of equations

$$\mathbf{QA} = \mathbf{RB} \tag{7}$$

and

$$\mathbf{SA} = \mathbf{PB}, \tag{8}$$

where

$$Q_{mn} = A_n U_n \frac{a h_{nu}}{h_{ms}^2 - h_{nu}^2} J_1(h_{ms}a) J_0(h_{nu}a) \sin(p_{nu}L), \tag{9}$$

$$R_{mm} = B_m V_m \frac{b^2}{2} J_0^2(h_{ms}b) \cos(p_{ms}\frac{d}{2}), \tag{10}$$

$$S_{nn} = A_n U_n p_{nu} \frac{a^2}{2} J_0^2(h_{nu}a) \cos(p_{nu}L), \tag{11}$$

and

$$P_{nm} = B_n V_m p_{Ns} \frac{a p_{ms} h_{nu}}{h_{ms}^2 - h_{nu}^2} J_1(h_{ms}a) J_0(h_{nu}a) \sin(p_{ms}\frac{d}{2}), \tag{12}$$

noting that both **R** and **S** are diagonal matrices.

The system of equations represented by (7) and (8) is rewritten as

$$[\mathbf{Z}][\mathbf{X}] = \mathbf{0}, \tag{13}$$

where

$$[\mathbf{Z}] = \begin{bmatrix} \mathbf{Q} & -\mathbf{R} \\ \mathbf{S} & -\mathbf{P} \end{bmatrix}, \tag{14}$$

and

$$[\mathbf{X}] = \begin{bmatrix} \mathbf{A} \\ \mathbf{B} \end{bmatrix}. \tag{15}$$

The resonance condition follows from the fact that this linear system of equations has a nontrivial solution only if

$$\det[\mathbf{Z}] = 0. \tag{16}$$

We can use (16) to iteratively calculate either the resonant frequency of the split-cylinder cavity given a known sample permittivity $\epsilon_s^{'}$, or the sample permittivity given a measured resonant frequency f.

LOSS TANGENT

In order to discuss the measurement of the sample loss tangent $\tan\delta_s$, we must first examine the definition of the measured quality factor Q of the split-cylinder resonator when a sample is present:

$$Q = \frac{\omega(W_a + W_s)}{P_e + P_f + P_w + P_s}, \tag{17}$$

where W_a and W_s are the average energies stored in the cylindrical cavity and sample regions, and P_w, P_c, P_f, and P_s are respectively the power dissipated per second in the cylindrical cavity endplate, walls, flange, and sample. Note that we have ignored the power dissipated in the coupling loops as we ensured that the resonance was very weakly coupled (<-50 db). When we calculate the sample permittivity using (16), we also determine the coefficients A_n and B_n, thereby allowing us to write the energy-stored terms as

$$W_s = \epsilon_0 \epsilon_s^{'} \int_{z=0}^{\frac{d}{2}} \int_{\rho=0}^{b} \int_{\phi=0}^{2\pi} |E_{\phi_s}|^2 \rho \, d\phi \, d\rho \, dz, \tag{18}$$

$$W_a = \epsilon_0 \epsilon_a^{'} \int_{z=\frac{d}{2}}^{L} \int_{\rho=0}^{a} \int_{\phi=0}^{2\pi} |E_{\phi_u}|^2 \rho \, d\phi \, d\rho \, dz, \tag{19}$$

and the power-dissipated terms as

$$P_e = R_s \int_{\rho=0}^{a} \int_{\phi=0}^{2\pi} |H_{\rho_u}|^2 \rho \, d\phi \, d\rho \, \Big|_{z=L}, \tag{20}$$

$$P_w = R_s \int_{z=\frac{d}{2}}^{L} \int_{\phi=0}^{2\pi} |H_{z_u}|^2 \rho \, d\phi \, dz \, \Big|_{\rho=a}, \tag{21}$$

$$P_f = R_s \int_{\rho=a}^{b} \int_{\phi=0}^{2\pi} |H_{\rho_s}|^2 \rho \, d\phi \, d\rho \, \Big|_{z=\frac{d}{2}}, \tag{22}$$

$$P_s = \tan\delta \, \omega \epsilon_0 \epsilon_s^{'} \int_{\rho=0}^{b} \int_{z=0}^{\frac{d}{2}} \int_{\phi=0}^{2\pi} |E_{\phi_s}|^2 \rho \, d\phi \, d\rho \, dz. \tag{23}$$

	Split-Cylinder Resonator			Cylindrical Cavity		
Sample	f (GHz)	$\epsilon_s^{'}$	$\tan\delta \times 10^{-4}$	f (GHz)	$\epsilon_s^{'}$	$\tan\delta \times 10^{-4}$
Fused Silica	8.673	3.85	1.3	8.676	3.84 ± 0.02	0.9 ± 0.5
Single-Crystal Quartz	8.785	4.46	0.2	8.787	4.45 ± 0.02	0.08 ± 0.5
Alumina	8.136	10.02	.02	8.087	9.99 ± 0.05	0.4 ± 0.5

Table 1: Comparison of measured permittivity and loss tangent between split-cylinder resonator and cylindrical cavity methods for four low-loss samples.

Given that $\epsilon_s^{'}$ is calculated from the measured resonant frequency, the two remaining unknown variables used to determine the energy stored and power dissipated are the surface resistivity R_s of the cylindrical waveguide sections and the loss tangent of the sample $\tan\delta$. We obtain R_s from a measurement of the quality factor of the empty split-cylinder resonator, where the gap between the cylindrical waveguide sections is closed. Then, after measuring the quality factor Q of the split-cylinder when the sample is present, we solve (17) for the sample loss tangent $\tan\delta$.

MEASUREMENT RESULTS

We used the split-cylinder resonator method to measure the complex permittivity of three low-loss dielectric samples: fused silica, single-crystal quartz, and alumina. The split-cylinder resonator was constructed from cylindrical waveguide sections, each having a diameter of 38.1 mm and length of 25.3 mm. Each section was constructed of oxygen-free copper and had a small hole in the waveguide wall for the coupling loop. Each sample, 60 mm in diameter, was placed between the two waveguide sections of the split-cylinder resonator, and the resonance curve for the TE_{011} mode was examined on an automatic network analyzer. From the resonance curve, we obtained the resonance frequency f and the quality factor Q. From these two quantities and the geometrical dimensions of the split-cylinder resonator and sample, we calculated the sample relative permittivity using (16) and the sample loss tangent using (17).

In order to verify these permittivity and loss tangent measurements made with the split-cylinder resonator, we compared them to measurements made with the cylindrical-cavity method [5]. Table 1 compares the measurements made in the split-cylinder resonator and cylindrical cavity for three different materials. The permittivity results for the split-cylinder measurements agree well with measurements made with the cylindrical cavity. Although the loss tangent results also agree, the uncertainties in the cylindrical cavity are relatively large, so it's difficult to draw conclusions about the accuracy of the loss tangent measurements from the split-cylinder resonator. We are currently investigating other techniques, with lower uncertainties in loss tangent, to better verify the measurement accuracy of the split-cylinder measurements of loss tangent.

CONCLUSIONS

Using the mode-matching method, we have developed a new model for measuring the permittivity and loss tangent of substrate materials by using the split-cylinder resonator method. By properly taking into account the fringing electric and magnetic fields, we have improved the measurement accuracy of this technique. To verify the new theoretical model, we compared permittivity and loss tangent measurements made in both the split-cylinder resonator and cylindrical cavity and found good agreement between the two methods.

REFERENCES

[1] G. Kent, "An evanescent-mode tester for ceramic dielectric substrates," *IEEE Trans. Microwave Theory Tech.*, vol. 36, no. 10, pp. 1451–1454, October 1988.

[2] G. Kent and S. Bell, "The gap correction for the resonant-mode dielectrometer," *IEEE Trans. Instrum. Meas.*, vol. 45, no. 1, pp. 98–101, February 1996.

[3] M. Janezic and J. Baker-Jarvis, "Full-wave analysis of a split-cylinder resonator for nondestructive permittivity measurements," *IEEE Trans. Microwave Theory Tech.*, vol. 47, no. 10, pp. 2014–2020, 1999.

[4] G. Eleftheriades, A. Omar, and L. Katehi, "Some important properties of waveguide junction generalized scattering matrices in the context of the mode matching method," *IEEE Trans. Microwave Theory Tech.*, vol. 42, no. 10, pp. 1896–1903, October 1994.

[5] E. Vanzura, R. Geyer, and M. Janezic, *The NIST 60-Millimeter Diameter Cylindrical Cavity Resonator: Performance for Permittivity Measurements*, Natl. Inst. Stand. Technol. Tech. Note 1354, 1993.